3rd URSI AT-AP-RASC, Gran Canaria, 29 May – 3 June 2022

# On the influence of the vertical variability on the Earth-to-satellite communication link rain retrievals

Elisa Adirosi[1], Luca Facheris[2], Filippo Giannetti[3], Fabiola Sapienza[3], Giacomo Bacci[3,4], Attilio Vaccaro[4], Alessandro Mazza[5], Alberto Ortolani[5] and Luca Baldini[1]

(1) Institute of Atmospheric Sciences and Climate, CNR, Rome, Italy
(2) Department of Information Engineering, University of Florence, Florence, Italy
(3) Department of Information Engineering, University of Pisa, Pisa, Italy
(4) M.B.I. s.r.l., Pisa, Italy
(5) Consorzio LaMMA and Institute for the Bio Economy (IBE) of the Italian National Research Council (CNR), Florence, Italy

## Abstract

In the last two decades, several studies exploited opportunistic microwave signals to improve precipitation estimation capability. In this framework, the Nefocast project developed an ad-hoc algorithm to retrieve precipitation from the attenuation experienced by Earth-to-satellite links and deployed an extensive field campaign to validate the algorithm. Thanks to the co-located measurements of a satellite receiver (SmartLNB), a disdrometer and weather radar in Rome, several assumptions of the Nefocast algorithm were addressed. Recently a vertically pointing micro rain radar (MRR-PRO) was added to the Rome set-up allowing the analysis of the variability of the precipitation and its possible influence within the Nefocast algorithm. The preliminary results showed that the vertical variability of precipitation can play a role in the Nefocast estimates.

## 1. Introduction

The use of opportunistic microwave (MW) communication links to obtain quantitative precipitation estimates has become a research topic that has gained growing interest in the last decades. Estimation of precipitation relies on the attenuation experienced by a MW signal due to the presence of precipitation along the propagation path. In fact, at the frequencies used by commercial MW links, attenuation is significant, caused mainly by the interaction of the wave with liquid and mixed-phase hydrometeors. For liquid precipitation, the relationship between the specific attenuation ($k$ , dB km$^{-1}$) and the rainfall rate ($R$ , mm·h$^{-1}$) is expressed through a power law $k= aR^b$ with coefficients depending on wave characteristics like frequency and polarization, and environmental parameters like temperature, particle types and density, and the size distribution of cloud and precipitation particles. In principle a rainfall rate estimate can be associated to a path attenuation measurement.

The use of tropospheric MW links of cellular communication networks to estimate precipitation, owing to a number of studies, has achieved a maturity level enabling operational implementations suited both for densely populated areas and for areas where operation rainfall measurement devices are scarce or absent [1]. More recent studies have targeted the use of attenuation measurements made along the satellite-to-ground links of communication satellites (typically geostationary satellites for direct TV broadcasting) to estimate precipitation. A review of such studies can be found in [2]. It should be noted that different approaches involving different kind of receivers can be considered [3]. Statistical validation studies performed with calibrated rain gauges [4] or ground based weather radar [5] and using different receivers have shown, in general, a good performance of rain retrieval algorithms. Methods to obtain rainfall maps using networks of receivers have been also proposed [6] [7]. As part of the validation program of the Nefocast project, funded by the Tuscany Region Government (Italy), a physical validation exercise [8] was performed to evaluate the influence of several factors affecting the performance of the rain retrieval algorithm described in [9]. An experimental setup was purposely deployed in Rome, where co-located with a SmartLNB receiver, installed were a laser disdrometer and a research grade dual-polarization weather radar (Polar 55C) pointing in the direction of the MW link. This configuration allowed to evaluate the impact of several assumptions of the retrieval algorithm, such as the adoption of a fixed $k$-$R$ relationship with regard to the variability related to changing drop size distribution, or the use of a height of the 0°C isothermal obtained from a numerical weather model instead of the height and thickness of the melting layer estimated in real-time from dual polarization weather radar that presents a high variability in time. Unfortunately, due to several factors, including the influence of ground clutter close to the radar site, radar measurements close to the radar were not usable to evaluate the impact of vertical variability on rain retrieval, whereas a constant vertical profile is assumed below the melting layer. Recently, a Micro Rain Radar (MRR) has been made available and placed next to the SmartLNB and the disdrometer to obtain a more accurate and detailed description of the vertical variability of

precipitation. This summary paper describes the preliminary results obtained with this experimental setup focusing the influence of vertical variability of precipitation on rainfall estimation with satellite-to-ground link.

## 2. Experimental setup

Fig. 1 shows the setup at the CNR-ISAC in Rome running since October 2021. Circled are the SmartLNB receiver (cyan), the Laser disdrometer (red) and the vertically pointing radar profiler (green). The experiments conducted with this setup started in November 2021. Subsections detail the instruments used.

### 2.1 SmartLNB

The SmartLNB manufactured by AYECKA Ltd. (Israel) was tuned on 11.3458 GHz for the forward link (i.e, sat-to-ground) and on 14.2166 GHz for the return link (ground-to-sat) using the Eutelsat 10-A geostationary broadcast satellite, located at 10° E. The elevation angle in Rome is 41.8°.

The terminal provides time series of the instantaneous value of the ratio between the average RF energy per symbol and the one-sided power spectral density of the channel noise (Es/N0). Using this information and the additional information about the 0°C height, the algorithm described in [9] extracts the component of attenuation due to precipitation using a double Kalman filter followed by an inversion model based on a climatologically tuned *k-R* relationship and the melting layer model in [12].

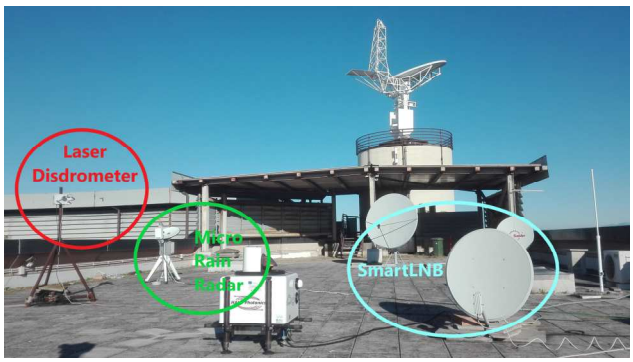


**Figure 1:** Experimental set-up on the roof of ISAC-CNR in Rome. Circled are the instruments involved in the experiment.

### 2.2 Laser Precipitation Monitor

The disdrometer on the roof of ISAC-CNR is the laser disdrometer manufactured by Adolf Thies GmbH called Laser Precipitation Monitor. Every minute, it records the number of particles that fall through its detection area of 46.5 $cm^2$. The particle diameter classes range between 0.125 and 8 mm, while the fall velocity ranges between 0.2 and 10 $m \cdot s^{-1}$. From a drop count matrix, the drop size distribution (DSD), and their integral parameters (such as the rainfall rate), can be computed. A filter criterion is adopted to filter out spurious drops and to mitigate the errors due to environmental factors, mainly the wind. In particular, the drops with measured velocities outside ±50% of a given raindrops fall velocity are removed from the set.

### 2.3 MRR Pro

MRR-PRO is a K-band (24 GHz), Doppler, FMCW profiling radar manufactured by Metek GmbH. It follows the older MRR-2 (MRR stands for Micro Rain Radar), a device characterized by a relatively affordable price, easily deployable and robust so that has been adopted in many experimental campaigns for liquid [10] and ice precipitation measurements, also in extreme environmental conditions [11]. With respect to its predecessor, MRR-PRO, allows more flexibility in the choice of acquisition parameters. In this study the resolution is 35 m and all the geophysical retrievals are obtained using the software provided by the manufacturer. The first bin is at 120 m above ground level.

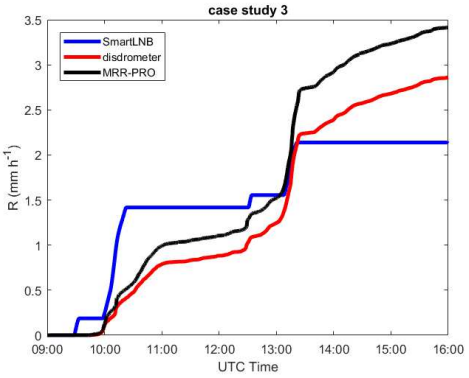


**Figure 2:** example of event cumulated rainfall rate obtained by SmartLNB, disdrometer and MRR PRO.

As example, Fig. 2 shows the event-cumulated rainfall obtained during 26 December 2021 from SmartLNB, disdrometer and MRR-PRO at the lowest reliable bin (i.e. 155 m above the ground level). Observed is a stratiform long lasting (i.e 6 hours) event with almost light precipitation (i.e. lower than 10 mm $h^{-1}$) except for few peaks up to 15 mm $h^{-1}$ recorded by the MRR-PRO. Although the different measuring principles and sampling volumes, the agreement among the different devices is good, in particular for the first part of the event. The difference of the total cumulated rainfall at the end of the events is mainly due to the different estimation of the peak occurred for a few minutes around 13:30 UTC.

## 3. Vertical variability of precipitation

One of the main assumptions of the Nefocast algorithm [9], that allows to retrieve rainfall rate from the values of Es/N0 recorded by the SmartLNB, is that the precipitation is constant along the earth-to-satellite path in the liquid layer (i.e., between the SmartLNB and the bottom of the melting layer, ML).

Assuming that the variability of precipitation along the vertical is like the one along the 41.8° elevation slanted path, the measurements provided by MRR-PRO can be

useful to investigate the variability of the precipitation and the possible influence on the Nefocast rain retrievals.

In this preliminary analysis, three stratiform events occurred on 01, 11 and 26 December 2021 have been considered. Fig. 3 shows the radar reflectivity factor registered by the MRR-PRO along the vertical during the latter events, furthermore the height of the bottom (red line) and of the top (black line) of the ML have been reported. The maximum range of the MRR-PRO is around 4.5 km above the ground level. The ML has been detected around 2 km for two cases study and a bit lower for the third one. The variability of the precipitation in the liquid layer is evident, in particular for the case study 2 and for the more intense phases of the precipitation.

In order to quantify this variability, Fig. 4a shows the scatterplot between the rainfall rate at ground (namely *R*0) and the mean value of the rainfall rate within the liquid layer (namely above the ML). The best fit lines for the three events have a slope that range between 0.5 and 1.5 indicating a certain difference between the rainfall rate at ground and the mean value along the vertical. The case study 2 is the one with the highest slope but with the less dispersion of the data along the best fit line. In terms of error, the Root Mean Square Error (RMSE) values for the three events are: 4.9 mm $h^{-1}$, 0.4 mm $h^{-1}$ and 0.7 mm $h^{-1}$, respectively. The high values of RMSE for the first case study are likely due to the high dispersion of the data. However, the Normalized Mean Square Error for the three events are below 0.6 (namely 0.56, 0.61 and 0.45 for the first, second and third event, respectively).

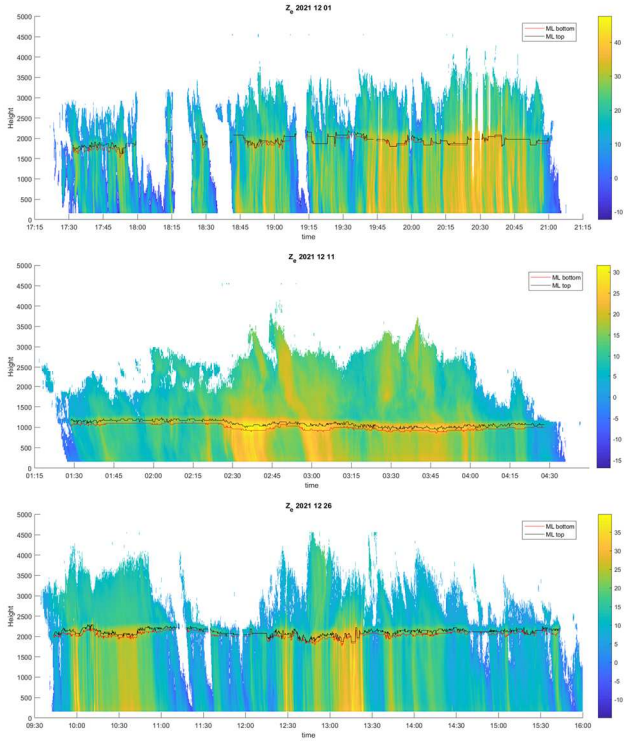


**Figure 3:** Time series of the reflectivity factor along the vertical for three case studies occurred on December 2021. Red lines represent the top of the ML, while black lines represent the bottom of the ML.

In the Nefocast algorithm, the signal to noise ratio (SNR) in wet and dry conditions are used to obtain the attenuation due to the precipitation, $L_{rain}$, (namely the one due to drops in the liquid layer and melted hydrometeors in the ML) [8]. For each instant $t$, knowing the $L_{rain}$, the corresponding rainfall rate $R_{LL}$ is estimated by solving the following equation

$$L_{rain}(t) = \overbrace{\alpha_{ML}[R_{LL}(t)]^{\beta_{ML}}\left[\frac{\delta_{ML}}{(\beta_{ML}+1)\sin\theta_e}\right]}^{ML\ contribution} - \underbrace{\alpha_{LL}[R_{LL}(t)]^{\beta_{LL}}\left[\frac{h_0-\delta_{ML}}{\sin\theta_e}\right]}_{LL\ contribution} \quad (1)$$

where the values of the coefficients ($\alpha_{LL}$, $\beta_{LL}$, $\alpha_{ML}$, and $\beta_{ML}$) are supposed to be constant. In the LL, the Ku-band coefficients ($\alpha_{LL}$ = 0.0153 and $\beta_{LL}$ =1.2531) have been obtained from a long time series of disdrometers data collected in Rome [9]. In the ML, we set $\alpha_{ML}$ = 0.01914 and $\beta_{ML}$ =1.1068, as in [12]. Assuming a uniform distribution of the rainfall rate, $R_{LL}$ is the rainfall rate at ground, $h_0$ is the height of the 0°C isotherm, $\delta_{ML}$ is the thickness of the ML and $\theta_e$ is the elevation angle that for Rome is 41.8°.

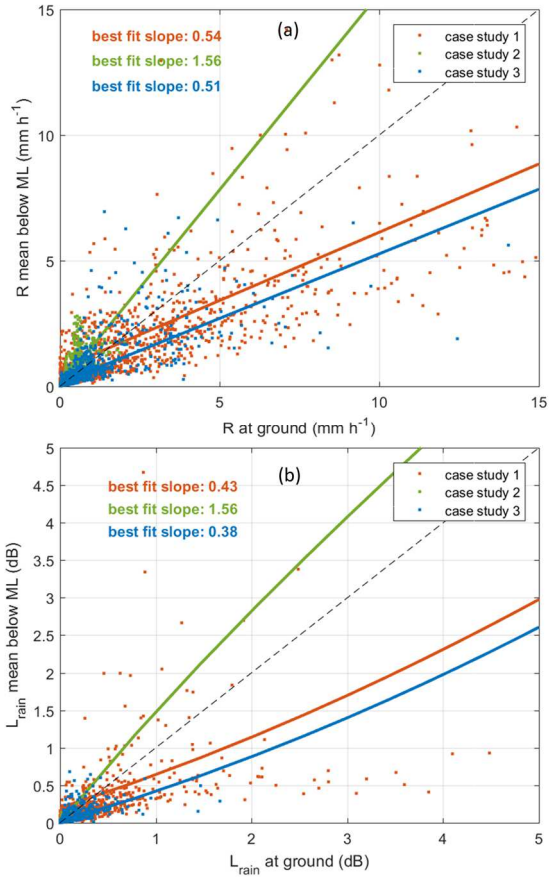

**Figure 4:** (a) scatterplot of the rainfall rate at ground vs the mean values of the rainfall rate in the liquid layer. (b) as (a) but for the attenuation of the precipitation.

In order to evaluate the effect of the precipitation variability on the attenuation, Fig. 4b shows the scatterplot of the $L_{rain}$ in dB obtained considering $R_{LL} = R0$ and $R_{LL} = R_{mean}$, namely the mean value of the rainfall rate below the ML. The obtained slopes of the best-fit lines are similar to the ones obtained for the rainfall rate comparisons (Fig. 4a). The RMSE are 0.70 dB, 0.02 dB, 0.07 dB, respectively for the three cases study, while the errors in terms of NMAE are less than 0.75.

## 4. Conclusions and future prospective

As follow up of a previous study presented in [8], this summary paper presents a preliminary analysis aimed at investigating the effects of the rainfall variability on the estimation of rainfall rate from Earth-to-satellite link measurements. The analysis was possible thanks to the recent installation of an MRR-PRO collocated with the SmartLNB and the disdrometer on the roof of ISAC-CNR in Rome. Preliminary results show that, within a stratiform event, the vertical variability of the precipitation can be relevant with a difference between rainfall rate at ground and the mean rainfall rate below the melting layer up to 60%. Similar differences are obtained in terms of $L_{rain}$, namely the attenuation due to precipitation considered in the Nefocast algorithm to estimate rainfall rate. Further analysis is needed in order to better quantify the effects of the precipitation variability on the Nefocast estimates and to consider more case studies that cover different type of events. In that regard, within the Insiderain project a multi-satellite rain sensor [3] will be installed on the roof of ISAC-CNR and will provide further data to investigate the performance of the retrieval of precipitation from Earth-to-satellite links.

## 6. Acknowledgements

This work was partially supported by the project INSIDERAIN (INStruments for Intelligent De-tection and Estimation of Rain for Agricultural INnovation) funded by Tuscan Region (Italy), Decreto n. 21885, 18 December 2020, and by the project SCORE (Smart Control of the Climate Resilience in European Coastal Cities) funded by European Commission's Horizon 2020 research and innovation programme under grant agreement No. 101003534. The project PER-ACTRIS (PIR01_00015), and APRA Piemonte are acknowledged for the availability of the MRR-Pro and the Laser disdrometer, respectively.

## References

1. L. de Vos, *et al.*, "Rainfall Estimation Accuracy of a Nationwide Instantaneously Sampling Commercial Microwave Link Network: Error Dependency on Known Characteristics," *J Atmos. Ocean. Technol.*, **36**, 7, Jul 2019, pp. 1267-1283. doi: 10.1175/JTECH-D-18-0197.1.

2. F. Giannetti and R. Reggiannini, "Opportunistic Rain Rate Estimation from Measurements of Satellite Downlink Attenuation: A Survey," *Sensors*, **21**, p. 5872, Aug 2021. doi: 10.3390/s21175872.

3. F. Giannetti *et al.*, Multi-Satellite Rain Sensor: Design Criteria and Implementation Issues., URSI AT-RASC 2022.

4. M. Colli, *et al.*, "Rainfall Fields Monitoring Based on Satellite Microwave Down-Links and Traditional Techniques in the City of Genoa," *IEEE Trans. Geosci. Remote Sens.*, **58**, 9, Sept. 2020, pp. 6266-6280, doi: 10.1109/TGRS.2020.2976137.

5. C. H. Arslan, K. Aydin, J. V. Urbina and L. Dyrud, "Satellite-Link Attenuation Measurement Technique for Estimating Rainfall Accumulation," *IEEE Trans. Geosci. Remote Sens.*, **56**, 2, Feb 2018, pp. 681-693 doi: 10.1109/TGRS.2017.2753045.

6. A. Ortolani, *et al.*, "An EnKF-Based Method to Produce Rainfall Maps from Simulated Satellite-to-Ground MW-Link Signal Attenuation," *J. Hydrometeorol.*, **22**, 5, May 2021, pp. 1333-1350, doi: 10.1175/JHM-D-20-0128.1.

7. L. Csurgai-Horváth, "Small Scale Rain Field Sensing and Tomographic Reconstruction with Passive Geostationary Satellite Receivers," *Remote Sensing*, **12**, p. 4161, 2020. doi: 10.3390/rs12244161.

8. E. Adirosi, *et al.*, "Evaluation of Rainfall Estimation Derived from Commercial Interactive DVB Receivers Using Disdrometer, Rain Gauge, and Weather Radar," *IEEE Trans. Geosci. Remote Sens.*, **59**, 11, Nov. 2020, pp. 8978-8991, doi: 10.1109/TGRS.2020.3041448.4

9. F. Giannetti, *et al.*, "Real-Time Rain Rate Evaluation via Satellite Downlink Signal Attenuation Measurement," *Sensors*, **17**, Aug. 2017, p. 1864, doi: 10.3390/s17081864.

10. E. Adirosi, L. Baldini, and A. Tokay, "Rainfall and DSD Parameters Comparison between Micro Rain Radar, Two-Dimensional Video and Parsivel2 Disdrometers, and S-Band Dual-Polarization Radar," *J. Atoms. Ocean. Technol.*, **37**, 4, Apr 2020, pp. 621-640. doi: 10.1175/JTECH-D-19-0085.1

11. A. Bracci, et al., "Quantitative Precipitation Estimation over Antarctica Using Different Ze-SR Relationships Based on Snowfall Classification Combining Ground Observations," *Remote Sensing*, **14**, 1, 2022, p. 82. doi: /10.3390/rs14010082

12. A. Dissanayake and N. McEwan, "Radar and attenuation properties of rain and bright band", in *Proc. Int. Conf. Antennas Propag.*, London, England, 1978